# Modified Nanoparticle Films for Transmission Plasmon Biosensing

K. Bonroy[*], F. Frederix[*#], G. Reekmans[*], H. Jans[*§], K. Jans[*§], B. Van de Broek[*§], R. De Palma[*§], C. Bartic[*] and G. Borghs[*]

[*] Interuniversity MicroElectronics Centre (IMEC), Kapeldreef 75, B-3001 Leuven, Belgium, bonroyk@imec.be, +32-16-281050
[§] KULeuven, Department of Chemistry, Celestijnenlaan 200F, B-3001 Leuven, Belgium
[#] Current Address: DSM, Research Campus, Urmonderbaan 22, 6160 MD Geleen, The Netherlands

## ABSTRACT

The principle of the Transmission Plasmon Biosensor (TPB) is based on the Localized Surface Plasmon Resonance (LSPR) properties of noble metal nanoparticles attached to a transparent substrate. When the analyte of interest binds to the biological receptor molecules immobilized onto these nanoparticles, the absorption of the nanoparticles will change due to local changes in the refractive index (RI). In this study, we investigated various parameters in order to increase the final sensitivity of the TPB such as the deposition method, the size, the material and the (bio)functionality of the nanoparticles. For biosensing applications, the nanoparticles were further functionalized with the desired biological receptor molecules (e.g. antibodies or ampicillin) using mixed Self-Assembled Monolayers (SAMs) [1]. In this paper, the experimental results on the modification and the characterization of the nanoparticle films will be presented together with the preliminary results on biological sensing.

***Keywords***: TPB, Nanoparticles, LSPR, Self-Assembled Monolayers, Biosensing

## 1 INTRODUCTION

Due to their interesting electromagnetic properties, noble metal nanoparticles such as Ag and Au have been the subject of intensive studies in diverse areas such as catalysis, optics, electronics and sensing devices. Their unique size-dependent properties are derived from the collective oscillations of the conduction electrons upon interaction with electromagnetic radiation, the so-called LSPR. The LSPR absorption band of nanoparticles, which can easily be visualized using transmission absorption spectroscopy, depends on different parameters such as the size and the shape of the particles, the material, the particle-particle interactions and the local environment including substrate, solvent and adsorbates. In various studies, the latter two optical properties have been extensively explored for sensing applications using both nanoparticles in suspension or nanoparticle arrays attached to a transparent substrate [2-4].

For the formation of such nanoparticle arrays, a variety of methods have been described including evaporation of gold islands, immobilization by covalent attachment at the surface of SAMs, colloidal and e-beam lithography, and Langmuir Blodgett techniques [2-4]. Although various promising studies have been described using these different nanoparticle arrays as sensing substrates in TPB, there are still important limitations.

In this paper, we investigated various parameters of the nanoparticle films in order to increase the final sensitivity of the TPB system. Therefore, we synthesized spherical Au and Ag nanoparticles and core-shell (Au@Ag) structures to study the influence of the nanoparticle material and size on the TPB sensitivity. Also multi-layered nanoparticle films were evaluated. Subsequently, the most promising nanoparticle film was selected to perform preliminary biological experiments using two model systems.

## 2 MATERIALS AND METHODS

### 2.1 Materials

Sodium ampicillin, silver nitrate, vitamin C, sodium citrate, glycerol, hydrogen tetrachloroaurate (III) trihydrate ($HAuCl_4$), sodium borohydride ($NaBH_4$), ethanolamine, n-hydroxysuccinimide (NHS) and n-(3-diethylaminopropyl)-n-ethyl-carbodiimide (EDC) were purchased from Sigma-Aldrich. 2-(2-(2-(2-(2-(2-(11-mercaptoundecyloxy)ethoxy) ethoxy)ethoxy)ethoxy)ethoxy)ethoxyacetic acid (11-PEO-COOH) was purchased from Prochimia, while 2-(2-(2-(11-mercaptoundecyloxy) ethoxy)ethoxy)ethanol (11-PEO-OH) was synthesized based on the method described previously [1]. Ultrapure ethanol was obtained from Riedel-DeHaen. Sulfuric acid, nitric acid, hydrogen peroxide and hydrochloric acid were received from VWR. Prostate specific antigen (PSA) was from Scipac, while 3-mercaptopropyltrimethoxysilane was purchased from Gelest. The antibody (Ab) against PSA was obtained from Fujirebio Diagnostics, while the Ab directed against ampicillin (clone 19C9) was a kind gift from the Laboratory of Veterinary Immunology (R.U. Gent, Belgium). The high optical quality AT-cut quartz samples were purchased from Chintele Quartz Technology Co. Ltd.

### 2.2 Synthesis of the metal nanoparticles

The synthesis of Au nanoparticles was performed as described previously [5]. Briefly, a solution consisting of boiling 0.01 % (w/v) $HAuCl_4$ is prepared and mixed with

various amounts of sodium citrate 1 % (w/v). The addition of 2 ml, 0.89 ml or 0.40 ml of citrate solution to 50 ml of $HAuCl_4$ resulted respectively in Au nanoparticles of ~13 nm, ~22 nm and ~42 nm according to TEM measurements. Their absorption bands showed a maximum at wavelengths of 518 nm, 523 nm and 536 nm respectively.

The spherical Ag nanoparticles were prepared by adding 1 ml of 1 % (w/v) aqueous $AgNO_3$ to 100 ml of water under vigorous stirring, followed by the addition of 1 ml of 1 % (w/v) aqueous sodium citrate. After 1 minute, 1 ml of 0.0075 % (w/v) $NaBH_4$ was added. The solution was stirred for at least 5 minutes. A size of ~21 nm was determined usingTEM.

The core-shell nanoparticles (Au@Ag) were prepared starting from the Au nanoparticles of ~13 nm. A shell of Ag was plated around these cores. Briefly, 2.5 ml of 0.001 M Vitamin C and 2.5 ml of the Au nanoparticle suspension were added to 25 ml of water. To this mixture, 500 µl of freshly prepared 0.01 M silver nitrate was added under vigorous stirring. The red colored solution turned yellow-brownish after a few minutes, resulting in the formation of Au@Ag nanoparticles of ~20 nm with a maximum absorption band at ~410 nm.

## 2.3 Preparation of the nanoparticle films

The nanoparticle films were prepared on quartz substrates. Before the deposition of the nanoparticles, the substrates were cleaned in a freshly prepared piranha solution. Subsequently, the substrates were immersed in a 10 % (v/v) 3-mercaptopropyltrimethoxysilane solution in 95 % (v/v) ethanol. After 3 h of silane deposition, the samples were thoroughly rinsed with ethanol and dried with $N_2$. The cross-linking was promoted in an oven at 108 °C. Immediately after the silanization, the samples were immersed in the nanoparticle suspensions for at least 24 h. Afterwards, the nanoparticle-coated quartz substrates were thoroughly rinsed with water and dried with $N_2$. By repeating the above-mentioned steps of silanization, cross-linking and deposition of the nanoparticles in a cyclic fashion, multi-layered nanoparticles films could be obtained.

## 2.4 Characterization of the nanoparticle films

The nanoparticle films were characterized using AFM, TEM and UV/Vis absorption spectroscopy. The UV/Vis spectroscopy measurements were conducted on a Shimadzu UV-1601PC spectrophotometer in combination with a home-made cuvet system suitable to mount the nanoparticle coated quartz substrates. The AFM measurements were performed using a Nanoscope IV Dimension 3100 instrument from Digital Instruments in combination with silicon cantilevers to acquire the tapping-mode AFM images. The TEM images were obtained on a Philips CM12 instrument using an acceleration voltage of 120 kV.

The sensitivity of the nanoparticle films was assessed using solutions with various RI. Hereto, mixtures of water and 0 %, 10 %, 20 %, 30 %, 40 % and 50 % of glycerol were prepared. The changes in the absorption spectra of the various nanoparticle films in the different glycerol solutions were measured using UV/Vis absorption spectroscopy.

## 2.5 Biological sensing experiments

To allow biofunctionalization, the nanoparticle films were modified with SAMs of thiols. Hereto, the freshly prepared nanoparticle films were immersed for 1 h in a 5/95 (v/v %) mixture of 1 mM 11-PEO-COOH and 11-PEO-OH in ethanol. After the SAM deposition, the thiol-coated nanoparticle films were mounted in the home-made cuvet system. First, the nanoparticles films were stabilized in PBS or HBS buffer (pH 7.4) until a stable UV/Vis absorption signal was obtained. Subsequently, the COOH-groups of the SAMs were activated using a 1/1 mixture of 0.4 M EDC and 0.1 M NHS. After 15 minutes of activation, the desired receptor molecules (ampicillin or anti-PSA) or the control receptor molecules (i.e. non-specific Ab) were covalently attached in a suitable coupling buffer onto the activated surface. For the binding of ampicillin, 10 mM borate buffer pH 8.5 was used, while coupling of the Abs was performed in 10 mM acetate pH 5.5. Blocking of the surface was performed using 1 M ethanolamine. Subsequently, the binding of the complementary affinity ligand (i.e. anti-ampicillin on ampicillin, and PSA on anti-PSA) was performed in HBS or PBS for 28 or 190 min. and monitored online via difference spectra using UV/Vis absorption spectroscopy.

# 3 RESULTS AND DISCUSSION

## 3.1 Preparation and characterization of the nanoparticle films

The quartz slides were modified with a thiol-based silane. This silane attaches to the oxide surface and leaves the -SH groups available for the covalent attachment of the Ag and Au nanoparticles via -S-Ag and -S-Au bonds. Using this method, we could successfully attach the different synthesized Au, Ag and Au@Ag nanoparticles as single nanoparticles films on top of the quartz slides resulting in homogeneous red- or yellow-colored films.

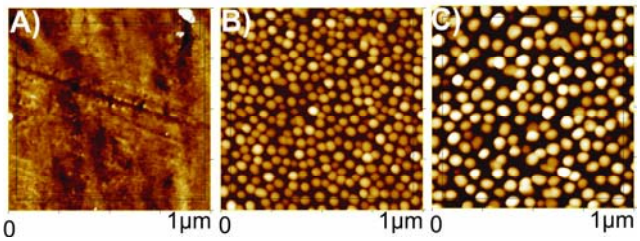


**Figure 1:** AFM images of the nanoparticles films. A) silane on quartz (z-range: 5.6 nm); B) ~20 nm Au nanoparticles on silanized quartz (z-range: 42.3 nm); C) ~42 nm Au nanoparticles on silanized quartz (z-range: 59.8).

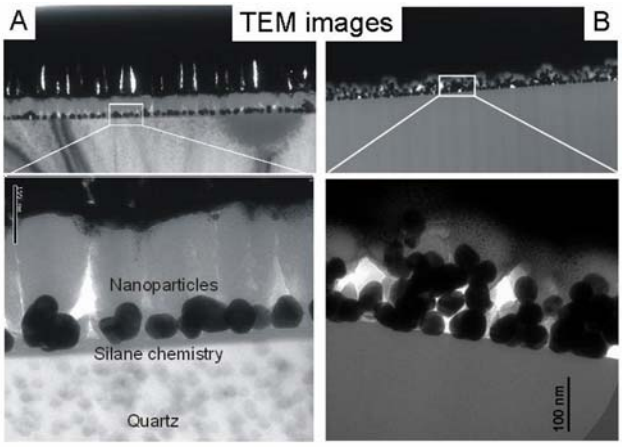


**Figure 2:** Cross-section TEM images of two nanoparticle films. A) Film of ~42 nm Au nanoparticles on silanized quartz; B) Multi-layered nanoparticle film of ~42 nm Au nanoparticles obtained after 5 deposition cycles.

Figure 1 shows the AFM images of a quartz slide coated with a silane layer and with Au nanoparticles of ~20 nm and ~42 nm. From these images it can be derived that the nanoparticles are not touching, but they form a sub-monolayer structure wherein the nanoparticles are separated a small distance from each other due to electrostatic repulsion. This is also clearly visualized using cross-section TEM (Figure 2-A).

Besides single-layered nanoparticle films, also multi-layered nanoparticle films could be obtained via repetitive silanization and nanoparticle deposition. Hereby, the silane layer acts as a cross-linker between the different gold nanoparticles. From the cross-section TEM images, we can clearly identify additional nanoparticles after repetitive deposition cycles (Figure 2-B). However, no clear stacking into well-organized multi-layered nanoparticle arrays could be observed.

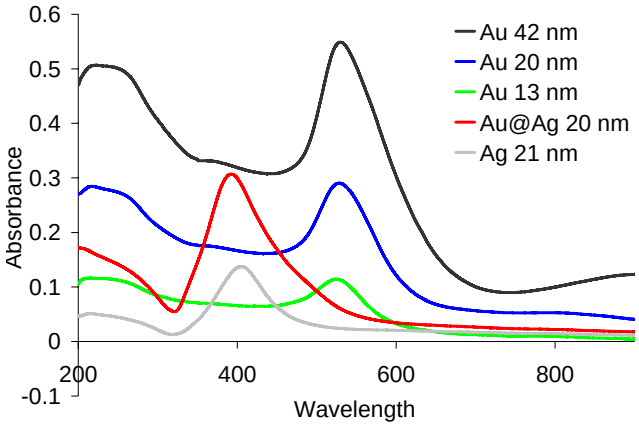


**Figure 3:** UV/Vis absorption spectroscopy of the nanoparticle films prepared using Au nanoparticles of 13 nm, 20 nm and 42 nm, Ag nanoparticles of 21 nm and Au@Ag of 20 nm (in water).

The optical properties of the nanoparticle films were investigated using UV/Vis spectroscopy (Figure 3). In the absorption spectra of the single-layered films of Au and Ag nanoparticles, one LSPR band can be distinguished at ~550 nm and at ~400 nm respectively. No distinct band was observed at higher wavelengths, indicating that no aggregation of the nanoparticles occurred in the single-layered nanoparticle films.

For the multi-layered nanoparticle films, a second broad absorption band at ~750 nm can be distinguished beside the one at ~550 nm (Figure 4). This band can only be attributed to plasmon coupling effects between the nanoparticles. Most likely, in our multi-layered films the silane acts as a shielding layer for the repulsive forces between the charged nanoparticles, allowing them to approach each other.

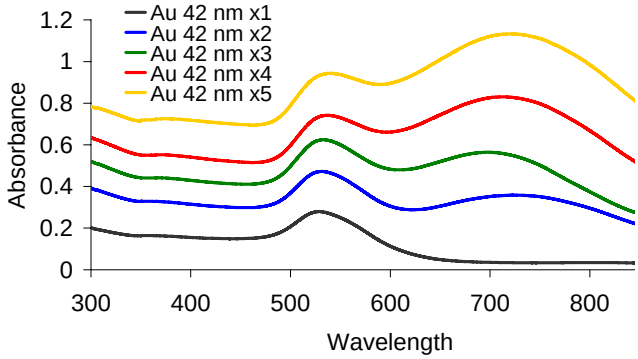


**Figure 4:** UV/Vis absorption spectra of the multi-layered nanoparticle films prepared using multiple depositions of Au nanoparticles of ~42 nm (in air).

Once the nanoparticle films were successfully fabricated, the sensitivity of the nanoparticle films was assessed. Hereto, the nanoparticle films were measured in glycerol solutions with increasing RI. Since the LSPR band of the nanoparticles is sensitive to local RI changes in their surrounding, the absorption band of the nanoparticle films shifted to higher absorption values and higher wavelengths (data not shown). By plotting these absorption and wavelengths shifts as a function of RI, linear calibration curves could be derived for the different nanoparticle films. The slope of these calibration curves are a measure for the sensitivity of the nanoparticle films (Table 1).

| | **Wavelength shift (nm)/ RIU** | **Absorption shift (AU)/ RIU** |
|---|---|---|
| Au 13 nm | 68.5 ± 8.9 | 0.216 ± 0.05 |
| Au 20 nm | 63.4 ± 9.0 | 0.450 ± 0.05 |
| Au 42 nm | 64.7 ± 7.1 | **0.775 ± 0.09** |
| Ag 21 nm | **91.4 ± 20.4** | 0.114 ± 0.170 |
| Au@Ag 20 nm | **102.8 ± 7** | 0.095 ± 0.06 |
| Au 42 nm x5 | **180.9 ± 60.4** | 0.447 ± 0.04 |

**Table 1:** Sensitivity of the nanoparticles films towards changes in refractive index units (RIU).

Firstly, we observed a higher sensitivity with the increasing size of the Au nanoparticles. Secondly, our

results suggested that the Au films are more sensitive in their absorption values, while the Ag films seem to be more sensitive in wavelength shifts. The core-shell Au@Ag nanoparticles behave similar to the Ag nanoparticles, suggesting that their sensing properties are not affected by the inner core. The multi-layered film also showed a high sensitivity in wavelength but the reproducibility was lower compared to the other films.

Due to its good reproducibility and high sensitivity in absorption, the Au 42 nm particle film was selected for further biological experiments.

## 3.2 Biological sensing experiments

For the preliminary biosensing experiments, the Au nanoparticles films were first modified with a mixed SAM incorporating poly-ethylene oxide (PEO) units. These PEO groups are known to reduce the non-specific binding [1]. The deposition of the thiol resulted in a shift of the LSPR band to higher wavelengths and absorption values (data not shown). Subsequently, the COOH-groups of the SAM were activated to allow covalent coupling of ampicillin or anti-PSA via their free $NH_2$-groups. The reference samples were either not coated with a receptor molecule or they were modified with a non-specific Ab. Blocking of the surface was performed to inactivate the NHS-esters and to reduce non-specific binding. After modification of the nanoparticle films with the receptor molecules, the specific affinity ligands were added to both the reference and the sample UV/Vis cuvets.

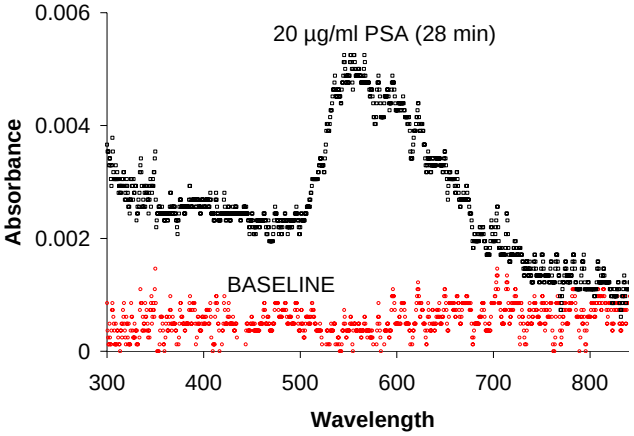


**Figure 5:** Difference absorption spectra of the binding of PSA onto the anti-PSA coated vs. a non-specific MAb coated nanoparticle film.

Due to the binding event that occurs between the analyte and the immobilized receptor molecule, the close environment of the nanoparticles changes. This should introduce a shift in the LSPR band of the specifically coated nanoparticle film.

Figure 5 shows the difference absorption spectra of the sample and reference nanoparticle films after addition of 20 µg/ml PSA followed by a buffer wash. The band around 550 nm in the difference spectra is attributed to the specific binding of PSA onto the anti-PSA coated nanoparticle film and the absence of binding onto the reference nanoparticle film coated with a non-specific Ab.

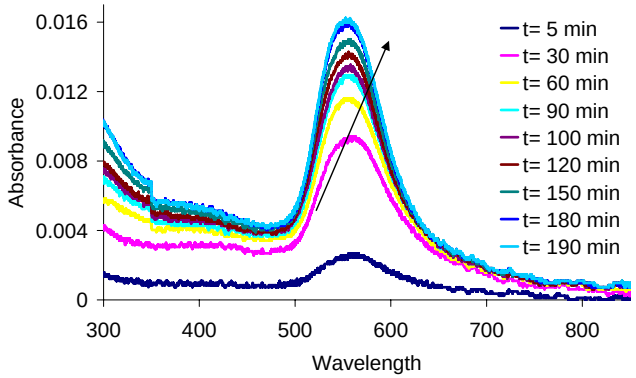


**Figure 6:** Difference absorption spectra of the binding of anti-ampicillin onto the ampicillin coated vs. a non modified nanoparticle film.

Similar as for the anti-PSA/PSA model system, the binding of the anti-ampicillin Ab onto a specifically coated ampicillin films was measured versus a non-coated nanoparticle film (Figure 6). Again, a clear band around 550 nm in the difference spectra is observed that can be attributed to the specific binding of the Ab to the ampicillin modified nanoparticle film. The higher binding signal in the ampicillin model system (0.009 vs. 0.005 absorption units after 30 min. contact time) can be explained by the small size of ampicillin molecules and hence the shorter distance at which the binding event takes place in this model system.

## 4 CONCLUSIONS

As a conclusion, various single- and multi-layered Au, Ag and Au@Ag nanoparticle films could be realized using self-assembly. Characterization of the films was performed using AFM, TEM and UV/Vis spectroscopy. In addition, the bulk sensitivity of the nanoparticle films towards changes in RI was investigated. Subsequently, the nanoparticle films were successfully modified with PEO-SAMs of thiols to covalently immobilize the biological receptor molecules (i.e anti-PSA Ab and ampicillin). Finally, the binding of the complementary affinity ligands was demonstrated.

## REFERENCES

[1] Frederix F. Bonroy K., Laureyn W., Reekmans G., Campitelli A., Dehaen W. Maes G., Langmuir, 19, 4351, 2003.

[2] Frederix F., Friedt J.-M., Choi K.-H., Laureyn W., Campitelli A., Mondelaers D., Maes G. and Borghs G., Analytical Chemistry, 75, 6894, 2004.

[3] Englebienne P., Van Hoonacker A., Verhas M., The Analyst, 126, 1645, 2001.

[4] Jensen T.R., Schatz G.C., Van Duyne R.P., Journal of Physical Chemistry, 103, 2394, 1999.

[5] Frens G., Nature Physical Science, 241, 20, 1973.